24th COBEM - 2017

24th ABCM International Congress of Mechanical Engineering
December 3-8, 2017, Curitiba, PR, Brazil

COBEM-2017-2099
NUMERICAL INVESTIGATION OF THE NEAR-FIELD ACOUSTIC LEVITATION APPROACH

Fábio Marques Ferreira Jr[1]
Geisa Arruda Zuffi[1]
fabio.ferreira@ufu.br, geisazuffi@ufu.br

Fran Sérgio Lobato
NUCOP – Laboratory of Modeling, Simulation, Control and Optimization, School of Chemical Engineering, Federal University of Uberlândia, Av. João Naves de Ávila, 2121, Uberlândia, MG, 38408-196, Brazil.
fslobato@ufu.br

Pedro Pio Rosa Nishida
LAV – Laboratory of Acoustics and Vibration, School of Mechanical Engineering, Federal University of Uberlândia, Av. João Naves de Ávila, 2121, Uberlândia, MG, 38408-196, Brazil.
pedronishida@ufu.br.

Aldemir Ap Cavalini Jr[1]
Valder Steffen Jr[1]
[1]LMEst – Structural Mechanics Laboratory, School of Mechanical Engineering, Federal University of Uberlândia, Av. João Naves de Ávila, 2121, Uberlândia, MG, 38408-196, Brazil.
aacjunior@ufu.br, vsteffen@ufu.br.

Abstract. *Levitation techniques have been attracting the attention of researchers in the last years, once they can be applied in the transportation, handling, and storage of components that cannot be contaminated by mechanical contact. Levitation is a process in which a force opposite to gravity is generated aiming to balance it without contact. Levitation can be achieved from electrical, magnetic, optical, aerodynamic, or acoustic forces. The present work is dedicated to the numerical analysis of the near-field acoustic levitation approach. In this case, the object is levitated due to forces generated by a pressure field produced from the vibration of a driving surface. The pressure field is obtained by solving the Reynolds equation. The influence that some parameters can exert on the pressure field is evaluated, such as the vibration amplitude of the driving surface and the so-called squeeze film number. In this paper, these parameters were analyzed in terms of the pressure amplitude that can be generated and the capacity of mass that can be levitated.*

Keywords: *Near-field acoustic levitation, squeeze film, Reynolds equation.*

1. INTRODUCTION

The acoustic levitation presents advantages over the other approaches, since it does not offer any restrictions to the chemical composition of the material desired to be levitated and does not require that it be electrified. For example, the acoustic levitation is able to be used even to levitate small animals (Vandaele et al., 2005; Andrade, 2010).

There are different acoustic levitation approaches reported in literature. The acoustic levitation based on flat waves is one of the simplest used techniques. This approach makes use of an ultrasonic transducer and a reflector, which is flat or curved. The waves generated by the transducer are reflected by the reflector on the transducer, forming waves with the same frequency that travels in opposite directions. The collision of these waves results in points of destructive and constructive interference (nodes and antinodes, respectively). In the nodes, the movement is null, generating a zone of low pressure. In contrast, in the antinodes one has areas of maximum pressure. As the objects tend to move from high pressure areas to low pressure areas, when the objects are placed between the transducer and the reflector among the created flat waves, they will move toward the nearest node and there they will remain (Hrka, 2015). Despite its simplicity, this technique presents some limitations. Once the low pressure zones exist only between the generated wave nodes, the object to be levitated can only measure half the length of the standing wave. Hence, only sound waves with

frequencies above 20KHz can be used to levitate macroscopic objects, requiring that the frequency generation must be precise (Castro, 2013).

Aiming to overcoming the limitations of the acoustic levitation approach based on flat waves, the near-field acoustic levitation (or ultrasonic levitation) can be used. This type of levitation occurs when a flat object is placed next to a vibrating surface. Consequently, there is a thin layer of air trapped into the gap between the driving surface and the flat object, which will be compressed due to the ultrasonic vibrations of the driving surface. Therefore, the levitation occurs due to the compression of the gas between the surfaces. The gas layer reaches an average pressure value higher than the ambient pressure, resulting in a force able of levitate the object above the vibrating surface (Ilsar et al., 2015). Thus, differently of the acoustic levitation based on flat waves, this technique does not restrict the size of the object.

In this context, this paper presents a preliminary study on the near-field acoustic levitation approach. For this aim, numerical simulations are performed to determine the influence of the system parameters on the levitation capabilities. It was considered a simplified system formed by a driving surface and an object of the same size and shape to be levitated by using the near field acoustic levitation technique. According to the literature presented, it was considered that the dynamics of the system can be determined through the Reynolds equation. This equation was numerically solved through the application of the finite centered difference technique. Different values for the amplitude of vibration of the driving surface (ε) and the squeeze number (σ) were considered, allowing to evaluate the influence of the same on the generated pressure field. Then, seven different mass values were considered to evaluate which combinations of ε and σ would be able to promote levitation.

2. PROBLEM DESCRIPTION

Figure 1 illustrates the problem to be evaluated, that consists of two discs at the same length, with a distance *h(t)* between them, and surrounded by atmospheric air at standard conditions. The lower disc, called driving surface, is responsible to create a pressurized gas film (with pressure $p(x, t)$), from an induced sinusoidal vibration on its surface with amplitude δh and frequency ω. Due to this, a force able of levitating the upper disc is generated. Besides that, the levitated object is subjected only to the pressure field and to the gravity. The system is considered symmetric and is solved in cartesian coordinates.

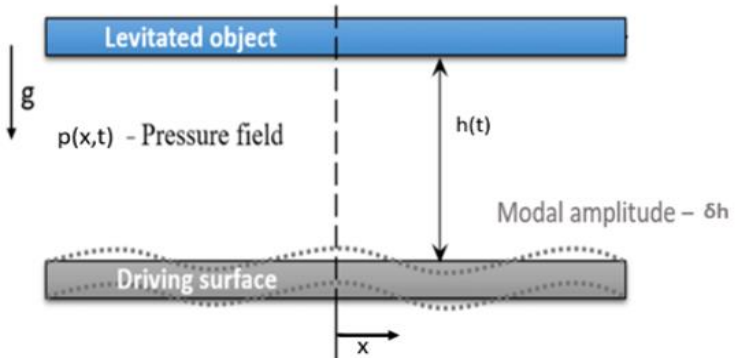

Figure 1: Graphic model of the system.

To simplify the analysis of the pressure field generated in this system, the object to be levitated will be considered fixed with a mean distance h_0 from the driving surface, which will be maintained oscillating in a sinusoidal form with amplitude δ_h and constant frequency ω. In this way, the gap between the discs can be represented by the Eq. (1).

$$h = h_0 + \delta h \, sin(\omega t) \tag{1}$$

3. Numerical Procedure

According to Zhao (2010), the air film behavior between the object and the action surface is represented by the Reynolds equation in cartesian coordinates presented by Eq. (2). In this analysis, it was assumed that the distance between the levitated and driving surfaces is small when compared to the other dimensions of the system. Additionally, the angular movement of the levitated object is disregarded and an isothermal boundary condition is considered.

$$\frac{\partial}{\partial x}\left(ph^3 \frac{\partial p}{\partial x}\right) = 12\mu \frac{\partial (ph)}{\partial t} \tag{2}$$

where p represents the pressure distribution that varies with the distance x and time t, h is the air gap, and μ is the dynamic viscosity of the air.

The Reynolds equation is solved in it dimensionless form. The non-dimension parameters are defined in Eq. (3).

$$P = \frac{p}{p_0}, H = \frac{h}{h_0}, X = \frac{x}{L}, T = \omega t, \sigma = \frac{12\omega\mu L^2}{p_0 h_0^2}, \epsilon = \frac{\delta h}{h_0} \tag{3}$$

where σ is defined as squeeze number, L is the characteristic length, p_0 is the atmospheric pressure and ε is the dimensionless vibration amplitude. So, the Eq. (1) and Eq. (2) can be rewritten as follows:

$$H = 1 + \epsilon\, sin(T) \tag{4}$$

$$\frac{\partial}{\partial X}\left(PH^3\frac{\partial P}{\partial X}\right) = \sigma\frac{\partial(PH)}{\partial T} \tag{5}$$

In Eq. (4), the parameter ε must be within the range $0 \leq \varepsilon \leq 1$ (Salbu, 1964). To obtain the profile of the pressure field in the gap, Eq. (5) should be solved numerically. In this paper, the finite differences method (centered approach) was applied to discretize the dimensionless Reynolds equation in N points, distant from each other by ΔX. Equation (6) presents the obtained Reynolds equation.

$$\frac{dP_i(T)}{dT} = \frac{P_i(T)}{H}\frac{dH}{dT} + \frac{H^2}{4X_i\Delta X^2\sigma}\left[(X_i + X_{i+1})(P_{i+1}^2 - P_i^2) - (X_{i-1} + X_i)(P_i^2 - P_{i-1}^2)\right] \tag{6}$$

where the subscript i indicates the discretization performed over the length x. In this case, it is assumed that the initial pressure in the gap is equal to the atmospheric pressure, as well as the pressure at the edge of the disc (Dirichlet boundary condition; see Fig. 1). In addition, symmetricity is imposed at the center of the disc. Thus, the pressure derivative is null at $x = 0$ (Neumann boundary condition). The considered initial and boundary conditions are presented in Eq. (7).

Initial condition: $P(X, T = 0) = 1$

Dirichlet boundary condition: $P(X = 0.5, T) = 1$ (7)

Neumann boundary condition: $\frac{\partial P(X=0,T)}{\partial X} = 0$

The pressure profile can be determined for different values of the σ and ε from Eq. (6) and Eq. (7). The obtained results will be presented in the next section.

4. RESULTS

Figure 2 presents the pressure profile in the gap between the object and driving surfaces for $\varepsilon = 0.5$ and $\sigma = 10$, 100, and 1000 (Fig. 2a, 2b, and 2c, respectively). Considering a simulation time of $T = 8$, $\sigma = 10$ results in a maximum pressure of $P = 1.6$ ($p = 0.16$ MPa). Note that the maximum pressure is located near the center of the gap and falls rapidly as it moves toward the edge of the disc. For $\sigma = 100$, the maximum pressure was $P = 1.7$ ($p = 0.17$ MPa), in which this value remained almost constant along the discs, decreasing only for $x > 0.4$. For $\sigma = 1000$, a different behavior is observed. Note that the maximum pressure $P = 3$ ($p = 0.30$ MPa) was obtained near the edge of the discs ($x > 0.45$). For the region near to the center of the discs, $P = 1.5$ ($p = 0.15$ MPa).

Figure 3 shows the behavior of the pressure field simulated for $\sigma = 100$ and $\varepsilon = 0.01$, 0.5 and 0.9 (Fig. 3a, 3b, and 3c, respectively). It was observed that the pressure distribution along the gap became more uniform, beginning to go down close to the edge of the disc and showing a behavior similar to the one observed in the Fig. 2b. The uniformity of the pressure distribution in the gap is related to the value of σ, having ε little influence in this behavior. On the other hand, the value of ε exerts a great influence on the amplitude of the generated pressure field. Thus, the larger the value of ε, the larger the pressure field generated in the gap will be, and, consequently the amplitude of vibration of the driving surface. For $\varepsilon = 0.01$, the maximum pressure was $P = 1.005$ ($p = 0.10$ MPa). For $\varepsilon = 0.5$, $P = 1.75$ ($p = 0.17$ MPa) and for $\varepsilon = 0.9$, $P = 9$ ($p = 0.91$ MPa).

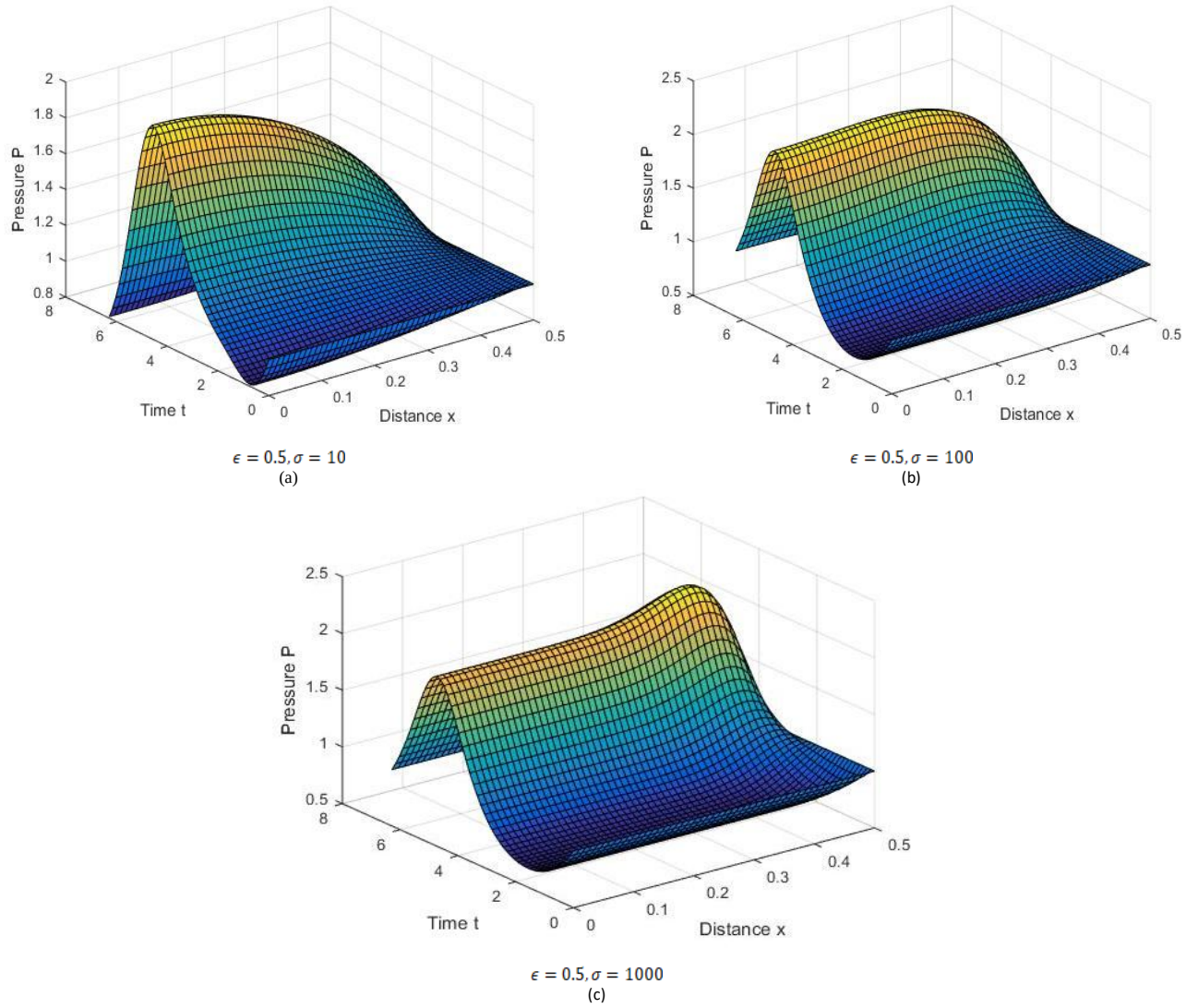

Figure 2: Pressure field in the gap varying with σ.

Figure 4 presents the maximum pressures obtained by changing both parameters ε and σ of the system. In this case, T = 8, 10 ≤ σ ≤ 1000, and 0 ≤ ε ≤ 1. Note that σ exerts small influence on the maximum pressure generated on the pressure field, which is highly dependent on the vibration amplitude of the driving surface (parameter ε). In the context of this analysis, it can be observed that the generated maximum pressure increases according to the vibration amplitude imposed on the driving surface for any value of σ within the considered range. Consequently, the levitation of the system is not associated with the excitation frequency applied by the driving surface.

Figure 5 summarizes the levitation capability of the presented approach in terms of ε and σ, considering different masses for the levitated object. In this case, masses of 100, 50, 20, 10, 1, and 0.2 kg are being evaluated (Fig. 5a to 5g, respectively) and T = 6.1221 (maximum pressures observed in Fig. 3 and Fig. 4) is considered for all the masses. The blue points represent the combinations of ε and σ in which can occur the acoustic levitation and the red ones in which it can't occur. For a mass of 100 Kg (Fig. 5a), the minimum value of ε necessary to occur levitation is 0.1 and the corresponding value of σ is 750. On the other hand, to occur levitation at the minimum value of the squeeze number (σ = 50), it is necessary to have ε > 0.4. As the mass decreases, the value of ε needed to promote levitation decrease as well and the system maintain the same behavior for the masses of 1, 0.2 and 0.05 Kg. Additionally, it can be observed that for all the analyzed masses, the levitation is achieved as σ decreases and ε increases.

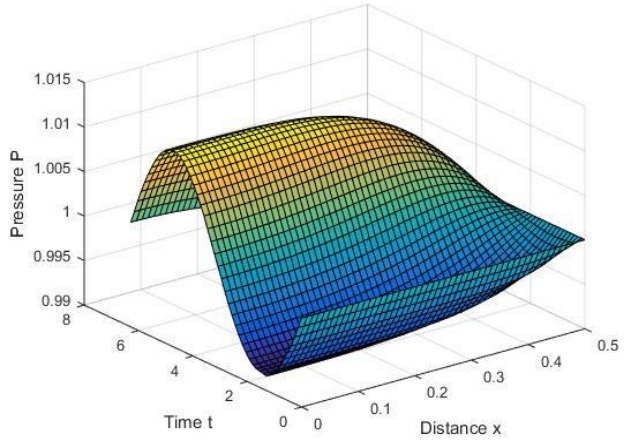

$\epsilon = 0.01, \sigma = 100$
(a)

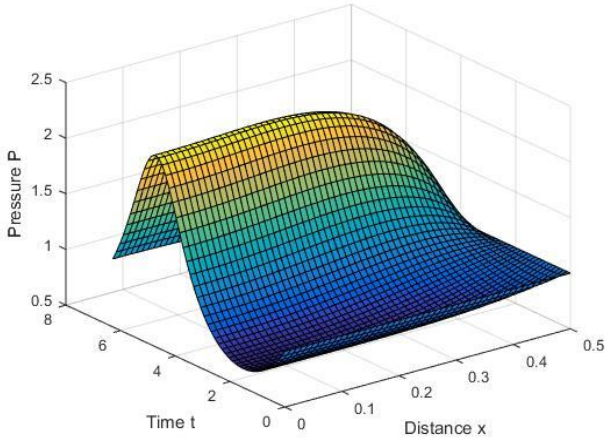

$\epsilon = 0.5, \sigma = 100$
(b)

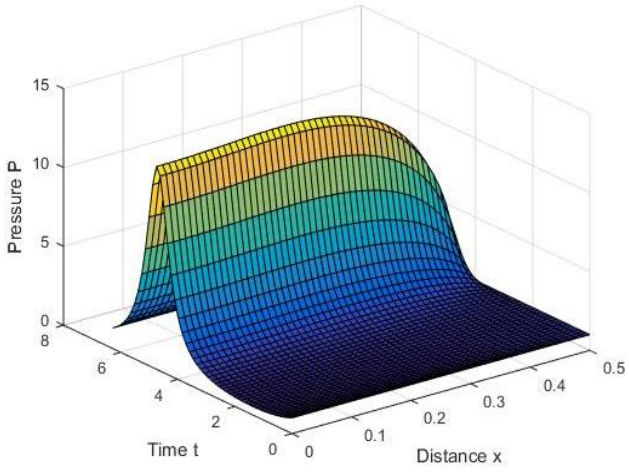

$\epsilon = 0.9, \sigma = 100$
(c)

Figure 3: Pressure field in the gap varying with ε.

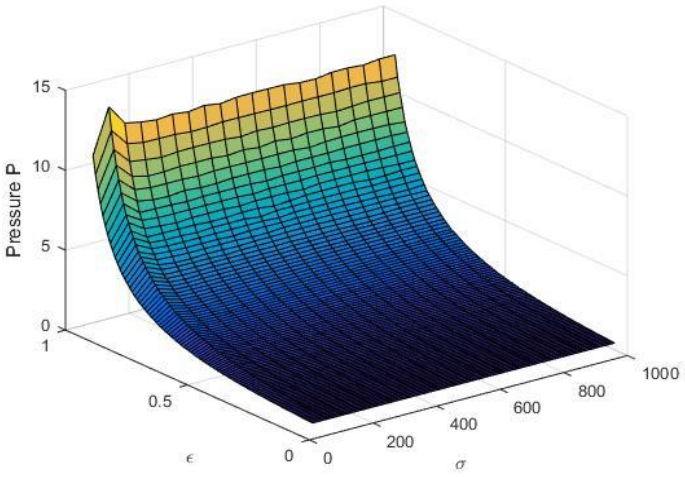

Figure 4: Maximum pressure field in the gap varying with ε and σ.

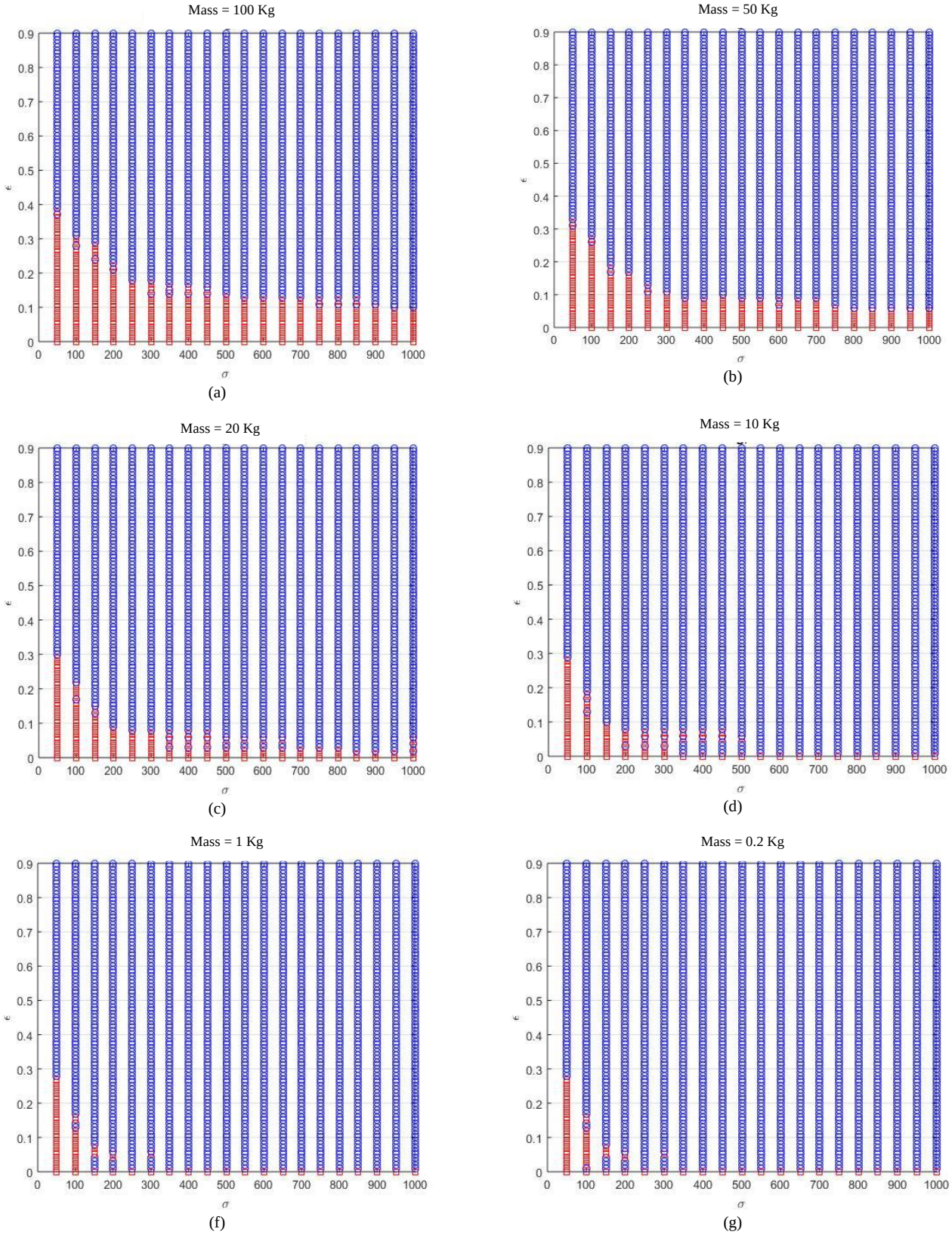

Figure 5: Possible combinations of ε and σ for levitation (the blue circles symbolize cases where there was enough force to levitate the object and red squares are associated to the no levitation condition).

5. CONCLUSION

In this paper, the near-field acoustic levitation approach was evaluated. The dynamic behavior of the system was determined through the Reynolds equation, which was numerically solved through the application of the finite

difference technique to obtain the pressure field generated between the levitated object and the driving disc. Different values for the parameters ε and σ were considered. The levitation capability of the presented approach was verified from objects with different masses for a range of ε and σ. It was possible to conclude that the maximum pressure generated between the discs increases according to ε. The parameter σ is related to the uniformity of the pressure distribution in the gap. Regarding the ability to generate a force able of promoting the acoustic levitation of the object, as expected, more combinations between ε and σ results in levitation as smaller is the mass of the object. Therefore, considering the scenarios investigated in this work, the obtained results are promising since they revealed the ability of the near-field acoustic levitation approach to levitate masses up to 100 kg. Further research effort will be dedicated to the experimental verification of the presented results.

6. ACKNOWLEDGEMENTS

The authors are thankful to the Brazilian Research Agencies CAPES, CNPq (574001/2008-5) and FAPEMIG (TEC-APQ-022284-15 / TEC-APQ-307609) for the financial support provided to this research effort.

7. REFERENCES

Andrade, M. A. B. *Estudo da força de radiação acústica em partículas produzida por ondas progressivas e estacionárias* (Doctoral dissertation, Universidade de São Paulo), 2010.

Castro, A. (2013). *Manipulation of biomimetic objects in acoustic levitation* (Doctoral dissertation, Université Pierre et Marie Curie-Paris VI).

E.O.J. Salbu. Compressible squeeze films and squeeze bearings. Journal of Basic Engineering, 86:355–366, 1964.

Hrka, S. Acoustic levitation. Seminar, University of Ljubljana, Faculty of Mathematics and Physics, 2015.

Ilssar, Dotan, and Izhak Bucher. "On the slow dynamics of near-field acoustically levitated objects under High excitation frequencies." *Journal of Sound and Vibration* 354 (2015): 154-166.

V. Vandaele, P. Lambert, A. Delchambre. *Non-contact handling in microassembly: acoustical levitation*. Precision engineering. 29 (2005): 491-505.

Zhao, S. (2010). *Investigation of non-contact bearing systems based on ultrasonic levitation* (Doctoral dissertation, Paderborn, Univ., Diss., 2010).

8. RESPONSIBILITY NOTICE

The authors are the only responsible for the printed material included in this paper.